

# The Role of an Aligned Nanofiber Conduit in the Management of Painful Neuromas in Rat Sciatic Nerves

Hede Yan, MD,\*† Feng Zhang, MD, PhD,‡ Chunyang Wang, MD, PhD,\* Zhen Xia, MD,\*  
Xiumei Mo, PhD,§ and Cunyi Fan, MD, PhD\*

**Background:** Capping techniques have been used as a treatment modality for the prevention of neuroma formation and the management of neuropathic pain. However, the results are inconsistent and unpredictable. We hypothesize that this situation may be attributable, in part, to the disparities in the type of materials used to manufacturing of the conduits.

**Methods:** In this study, a rat model was used and the sciatic nerve was selected for evaluation. In 1 capping group, a sciatic nerve stump was capped with a nonaligned nanofiber conduit (the nonaligned group), whereas in a second capping group, the conduit was made of aligned nanofibers (the aligned group). In another group, the sciatic nerve stump was not capped as a control (the control group). The results of autotomy behavior, extent of neuroma formation, histological changes in the neuroma, and the expression of c-fos as a pain marker in the fourth lumbar spinal cord were evaluated at 8 weeks postoperatively.

**Results:** The control group presented more neuroma-like features in all the observed parameters in comparison with the 2 capping groups; of the 2 capping groups, the aligned group achieved even better outcomes than the nonaligned group.

**Conclusions:** Our findings indicate that the aligned nanofiber conduit is a promising biomaterial for the nerve capping technique, and new treatment strategies using aligned nanofiber conduits may be developed for the management of painful amputated neuromas.

**Key Words:** capping technique, traumatic neuroma, neuroma prevention, aligned nanofiber nerve conduit, neuropathic pain

(*Ann Plast Surg* 2015;74: 454–461)

Injury of a peripheral nerve is often associated with the development of a posttraumatic neuroma, posing a significant challenge to surgeons.<sup>1</sup> Symptomatic neuromas occur in approximately 5% of patients who sustain a peripheral nerve injury. Furthermore, persistent pain occurs in approximately 60% of patients following limb amputation, and in 10% of such cases, the pain can be directly attributed to the formation of neuromas.<sup>2–4</sup> Pain related to neuroma formation is often resistant to nonsurgical treatments and can cause

serious morbidities, resulting in a high unemployment rate and high health care expenditures.<sup>5</sup>

Numerous techniques have been developed for the management of painful neuromas, with up to 150 approaches reported in the literature.<sup>6–12</sup> Despite a variety of treatment options, there is not yet a universally accepted method for the prevention of neuroma formation and the management of intractable pain from neuromas.<sup>13,14</sup> In the literature, there are 2 general categories of surgical interventions, namely shortening of the nerve or capping the nerve stump.<sup>15</sup> Nerve stump shortening can achieve very good clinical results in terms of pain relief; however, because of the natural tendency of recurrence of the neuroma at the new nerve transection site, long-term results can be unpredictable. Therefore, capping techniques have been developed as an alternative strategy in an attempt to cover the nerve stump with the goal of isolating it from the inflammatory cascade and neurotrophic factors that can lead to the recurrence of a painful neuroma. This procedure can be performed either by burying the nerve stump into a nearby anatomic structure or by capping it with either biological or synthetic materials, such as veins or silicone conduits.<sup>15–18</sup>

The management of traumatic neuromas using the capping technique is successful in some studies,<sup>15,17–19</sup> and it is theorized that its basic role is to create a mechanical barrier that isolates the nerve stump from the surrounding tissues.<sup>14,15</sup> However, the results of neuroma prevention and pain relief treated with different conduits are inconsistent and unpredictable.<sup>7,12,20</sup> Therefore, we hypothesize that the effectiveness of the capping technique depends not only on the conduit's ability to isolate the nerve from the surrounding structures but also on the inherent properties of the conduit. In this study, our objective was to investigate the role of aligned versus nonaligned nanofibers in the prevention of neuroma formation and the relief of pain.

## MATERIALS AND METHOD

### Preparation of the Nerve Conduits

Two types of nerve conduits were used (internal diameter, 2 mm): a nonaligned nanofiber conduit and an aligned nanofiber conduit. The nanofiber conduits were made of natural–synthetic polymeric nanofibers comprised of well-blended silk fibroin and poly(L-lactic acid-co-ε-caprolactone) by electrospinning in a weight ratio (RW) of 25:75. Our group has reported the fabrication of these nanofibers and addressed their biocompatibility and application in peripheral nerve regeneration after injury in our previous studies in rats.<sup>21,22</sup> All of the conduits used in this study were 12 mm in length.

### Animal Models and Grouping

Thirty-six male Sprague-Dawley rats weighing 250 to 300 g were used and randomly divided into 3 groups (n = 12, each): a control group, a nonaligned nanofiber conduit group (nonaligned group), and an aligned nanofiber conduit group (aligned group). All experiments were approved by the Institutional Animal Care and Use Committee, Shanghai Jiaotong University School of Medicine. Animals were treated according to the National Research Council's guidelines for the care and use of laboratory animals and had free access to rat chow and water.

Received February 6, 2014, and accepted for publication, after revision, April 10, 2014. From the \*Department of Orthopaedics, Shanghai Jiao Tong University Affiliated Sixth People's Hospital; †Department of Orthopaedics (Division of Plastic and Hand Surgery), The Second Affiliated Hospital & Yuying Children's Hospital of Wenzhou Medical University, Wenzhou, China; ‡Division of Plastic Surgery, University of Mississippi Medical Center, Jackson, MS; and §State Key Laboratory for Modification of Chemical Fibers and Polymer Materials, College of Materials Science and Engineering, Donghua University, Shanghai, China.

Conflicts of interest and sources of funding: This study was supported by funding from the National Natural Science Foundation of China (81171477), Key Project of Health Bureau of Shanghai (2012412), the Department of Education of Zhejiang Province (20051185), and Health Department of Zhejiang Province (201338025).

Reprints: Cunyi Fan, MD, PhD, Department of Orthopaedics, Shanghai Jiao Tong University Affiliated Sixth People's Hospital, 600 Yishan Road, Xuhui District, Shanghai, China, 200233. E-mail: fancunyi888@gmail.com.

Copyright © 2014 Wolters Kluwer Health, Inc. All rights reserved.

ISSN: 0148-7043/15/7404-0454

DOI: 10.1097/SAP.0000000000000266

## Surgical Procedure

Rats were anesthetized with pentobarbital sodium (50 mg/kg) given intraperitoneally. Under aseptic conditions, the right sciatic nerve was exposed between the biceps femoris and the gluteal muscles. To achieve a quantitative analysis of neuroma growth, the site giving off the branch of the posterior gluteal nerve was identified and carefully labeled with a 7-0 suture under a microscope. The sciatic nerve was then sharply transected 1 cm distal to the labeled site with the assistance of a 10-mm-long length marker. In all the cases, a gap of at least 15 mm was maintained distal to the transection site to avoid spontaneous nerve regeneration (Fig. 1). In the 2 capping groups, the proximal nerve stump was inserted 4 mm into the conduit and was sutured to the conduit with a single epineurial 11-0 monofilament nylon suture. In the control group, the proximal nerve stump was left in situ. In all groups, muscle wound beds and skin incisions were closed with 4-0 sutures, and ibuprofen analgesia was administered daily for 1 week after surgery.

## Animal Sacrificing Time and Specimen Preparation

Eight weeks after surgery, all the rats in each group were sacrificed by overdose of pentobarbital sodium followed by harvesting of the specimens. The proximal nerve stump was cut at the level of the marked site (the origin of posterior gluteal nerve) together with a 1-cm-long segment of normal nerve from the corresponding part of the contralateral side. Half of the specimens were randomly selected for histological evaluation ( $n = 6$ ). For the remaining 6 specimens, a 1- × 1-mm segment was first harvested in the center of the neuroma under the microscope for transmission electron microscope study, and the remaining tissue of these specimens was used for quantitative assessment of collagens I and III by Western blot analysis. The ipsilateral half of L4 spinal cord segment (positioned by the L4 nerve root) was also harvested for Western blot analysis of the expression of c-fos, which was used as a pain marker. All the specimens for the Western blot analysis were stored at  $-80^{\circ}\text{C}$ .

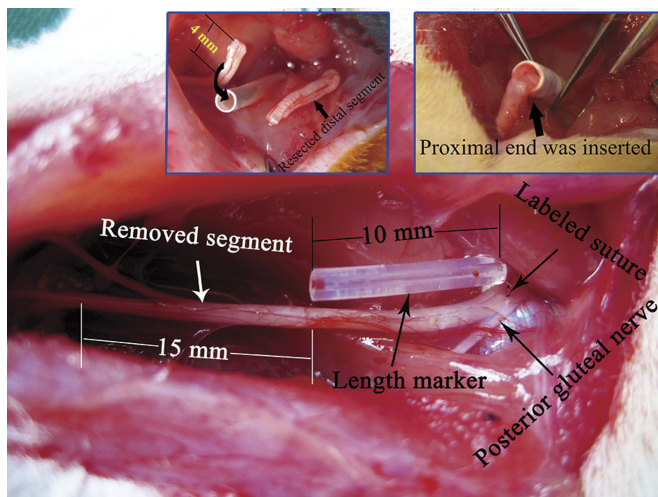


**FIGURE 1.** Demonstration of the animal model. The black arrows on the right show the site where the labeled suture was placed for quantitative analysis (top) and the origin of the posterior gluteal nerve (bottom); the arrow in the middle indicates the length marker (the silicone conduit in the middle) for accurate nerve cut. The white arrow on the left shows the nerve segment planned to be removed. The numbers 10 and 15 mm show the details of preparation of proximal nerve stump. The inset pictures on the top show the details of the capping procedure.

## Behavioral Analysis

The rats in each group ( $n = 12$ ) were monitored by dual, blinded observers for evidence of neuropathic pain for 8 weeks (autotomy scores recorded 3 times/wk). A modified Wall scale<sup>23</sup> was adopted to assign points according to the severity of autotomy. Briefly, 1 point was assigned for 2 or more toenails (maximum, 1 point per limb), and 1 point was assigned for each half digit (distal and proximal phalanges) for a possible maximum of 10 points per limb.

## Evaluation of Neuroma Growth

The neuroma growth was evaluated by a WR using the formula as follows: [the weight of neuroma (NW, after removal of the conduit) – the weight of the excised normal nerve segment (NNW)] / NNW.

## Histologic Analysis

The excised proximal stumps were first weighed and then processed by standard paraffin-embedding methods. Sections were cut at 4  $\mu\text{m}$ . To standardize the site for histological staining, the sections were randomly selected at a distance ranging from 400 to 600  $\mu\text{m}$  from the distal end of the specimens. At least 20 sections were obtained from each sample after the exclusion of small sections or poorly cut sections. Ten sections were randomly selected and 5 of the sections were used either for trichrome Masson's staining or labeled with antineurofilament (NF-200), respectively. Subsequent incubation with biotinylated secondary antibodies, horseradish peroxidase-conjugated avidin-biotin mixture, and chromagenic peroxidase substrate provided visualization of primary antibodies. The expression of NF-200 was detected with immunofluorescence method labeled with tetramethylrhodamine isothiocyanate. Three observation regions were randomly selected in each section, and the mean integrated optical density (OD) values measured by Motic Fluo 1.0 (Motic China Group Co., Ltd., Xiamen, China) were used for quantitative analysis. Chaotic arrangement of minifascicles was assessed semiquantitatively using a method similar to that proposed by Koch et al.<sup>24</sup> In brief, the specimens were graded from few (+) to many (+++) axons. All immunohistochemical supplies, including primary antibodies, were purchased from Sigma (Sigma, USA).

## Western Blot Analysis

The specimens were lysed with lysis buffer (100 mmol/L dithiothreitol, 50 mmol/L Tris-HCl, pH 6.8, 2% SDS, and 10% glycerol) containing protease inhibitors. The bicinchoninic acid method was used to determine the total protein concentration. Lysates with equal amounts of protein were resolved on sodium dodecyl sulfate polyacrylamide gel electrophoresis and then transferred to a polyvinylidene difluoride membrane. The membrane was then blocked in a solution containing tris-buffered saline (TBS), 0.05% Tween 20 and 3% nonfat dried milk (Bio-Rad Laboratories, Hercules, CA, USA) for 2 hours at room temperature with agitation. Subsequently, the membrane was incubated with primary antibodies diluted in blocking solution (mouse anti-c-fos 1:200, Santa Cruz Biotechnology, USA; mouse anticollagen type I 1:300, type III 1:200, Santa Cruz Biotechnology, USA). After washing in Tween 20 TBS containing TBS and 0.05% Tween 20, the membrane was then incubated at  $4^{\circ}\text{C}$  overnight with horseradish peroxidase-conjugated goat antimouse IgG (diluted 1:8000) in blocking solution. Anti- $\beta$ -Actin (1:8000, Santa Cruz Biotechnology, USA) was also added in this block solution as an internal loading control. The membrane was then washed with buffer, and the image was scanned with a GS800 densitometer scanner. OD data were analyzed using PD Quest 7.2.0 software using  $\beta$ -actin as the control.

## Transmission Electron Microscopy Study

The specimens harvested were immediately fixed in 2.5% glutaraldehyde in 0.1 M phosphate buffer overnight and then postfixed in osmium tetroxide 1%, stained with uranyl acetate, dehydrated in

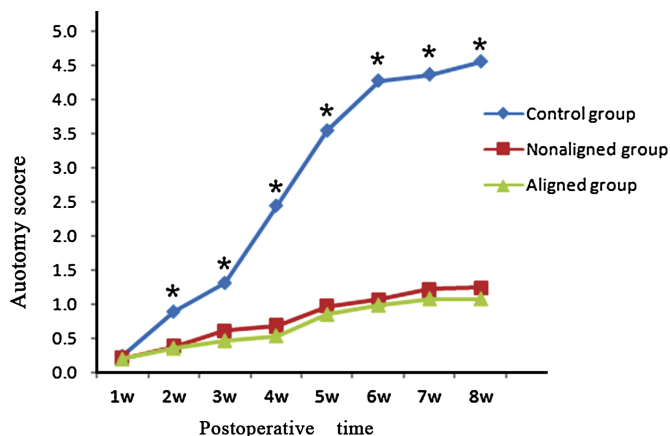


**FIGURE 2.** Results of weekly average autotomy scores. There was a statistically significant difference in autotomy scores between the control group and the other 2 capping groups at all of the time points except for the first week (all  $*P < 0.001$ ).

acidified 2,2-dimethoxypropane, and embedded in epoxy resin. Ultrathin sections (silver in color) of 70 nm were cut in an ultramicrotome (LKB 8800) and mounted on grids and examined in a transmission electron microscope. For quantitative analysis, photographs of each nerve sections were taken from 10 random fields. Morphometric indices, including the thickness of the myelin sheath and the ratio of unmyelinated and myelinated nerve fibers, were evaluated using Image J software. All measurements were performed by an investigator who was unaware of the grouping information of each section.

### Statistical Analysis

Nonparametric method of Mann-Whitney  $U$  test was used for the statistical analysis between groups using SPSS v. 19.0. For the autotomy score, repeated measures analysis of variance was used for calculating the overall significance of each curve and for comparison of data obtained at different periods after surgery among the groups of animals. The difference in the number of cases with autotomy between the 2 groups was compared using the  $\chi^2$  test. Fisher exact test was used for statistical analysis of the existence or absence of chaotically arranged minifascicles. Data were expressed as mean  $\pm$  standard deviations. Statistical significance was considered at the 5% level.

## RESULTS

### Autotomy Observation

The autotomy behavior was observed on the operated side in all animals. There was a statistically significant difference in autotomy scores between the control group and the 2 capping groups at all of the time points (both  $P < 0.001$ ) except for the first week (both  $P > 0.05$ ), and the autotomy scores were much higher in the control group than the other 2 groups after the first week, whereas no significant difference was revealed between the capping groups during the 8 weeks of observation (Fig. 2). In addition, the occurrence of autotomy in the control group was significantly higher than the other 2 groups (both  $P = 0.002$ ). Nine out of 12 control animals developed varying degrees of autotomy (autotomy score 3-6,  $4.95 \pm 0.81$ ), whereas only 2 rats in the nonaligned group and 1 in the aligned group showed evidence of autotomy behavior.

### Neuroma Growth

The WRs of neuromas of the 3 groups were  $1.60 \pm 0.087$ ,  $1.21 \pm 0.086$ , and  $0.91 \pm 0.135$ , respectively. A much higher WR was obtained in the control group compared with the other 2 groups

(both  $P < 0.001$ ), and the WR of the aligned group was even lower than that of the nonaligned group ( $P < 0.001$ ) (Fig. 3).

### General Observation and Histological Findings

In the control group, a typical bulbous neuroma was seen in 9 animals. In contrast, the nerve stumps in the nonaligned group progressively thinned out and terminated in a thin tissue strand, whereas a truncated nerve end was observed in the aligned group (Fig. 4).

Trichrome Masson's staining showed that highly proliferated collagen (stained in blue) was mingled with haphazardly arranged nerve fascicles in the control group (Fig. 5 above, middle), whereas only slightly blue stained collagen and orderly arranged nerve fibers were seen in the aligned group (Fig. 5 below, right). In the nonaligned group, the density of proliferated collagen was between the control group and the aligned group, but the collagen fibers were also distributed in a similar manner as that in the control group (Fig. 5 below, left). Quantitative study using Western blot assay further demonstrated that the highest expression of collagens I and III was seen in the control group and the lowest expression in the aligned group. The differences among the 3 groups in the content of types I and III collagen were all significant (all  $P < 0.001$ ) (Fig. 6).

The immunofluorescent staining study revealed that the nerve fibers in the stump labeled by NF-200 in the control group were densely dispersed in a chaotic manner with innumerable tiny bifurcations (Fig. 7 above, middle); in contrast, in the nonaligned group, the nerve fibers regenerated moderately but also presented a chaotic appearance (Fig. 7 below, left). However, the axons regenerated in the aligned group were distributed regularly and loosely in a linear fashion (Fig. 7 below, right). Minifascicles that coursed chaotically through the tissue were observed in both the control group and the nonaligned group, and no difference was observed between the 2 groups ( $P = 0.699$ ), whereas chaotically arranged minifascicles were not seen in the aligned group (both  $P = 0.002$ ). The average OD values of the 3 groups were  $0.486 \pm 0.012$ ,  $0.414 \pm 0.021$ , and  $0.237 \pm 0.013$ , respectively. The differences were significant among all the groups (all  $P < 0.001$ ) (Fig. 8).

### C-fos Expression in the Ipsilateral L4 Segment of Spinal Cord

The expression level of c-fos in the control group, nonaligned group, and aligned group was  $52.04 \pm 10.2$ ,  $31.71 \pm 5.55$ ,

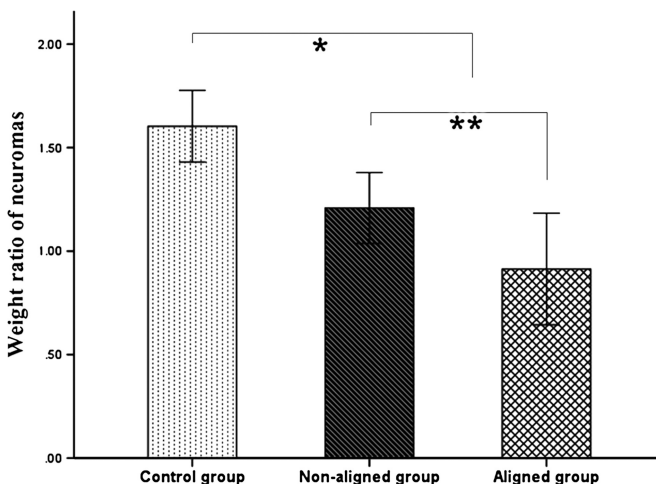


**FIGURE 3.** Results of weight ratio of neuromas. The weight ratio was the highest in the control group than the other 2 groups ( $*P < 0.001$ ), and the aligned group had a much lower weight ratio compared with the nonaligned group ( $**P < 0.001$ ).

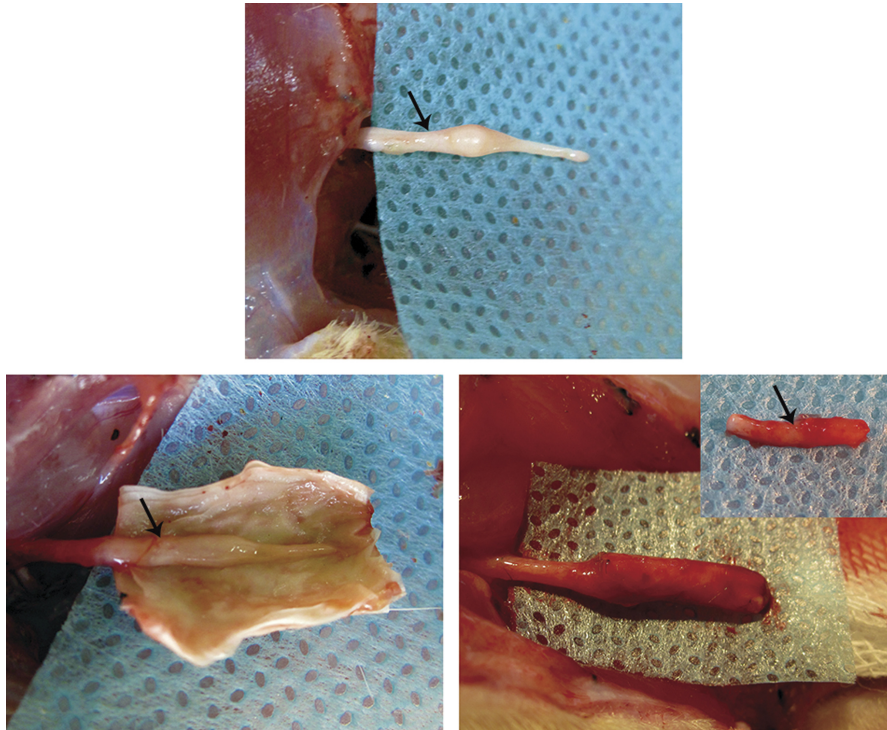


**FIGURE 4.** Neuromas appearance at 8 weeks after surgery. The arrow indicates the junction of the normal nerve and the start of the neuroma. (Above, middle) Appearance of a bulb-like neuroma in the control group. (Below, left) Appearance of a cone-shaped neuroma in the nonaligned nanofiber group. (Below, right) Appearance of neuroma with a truncated end in the aligned nanofiber group (the inset on the right top).

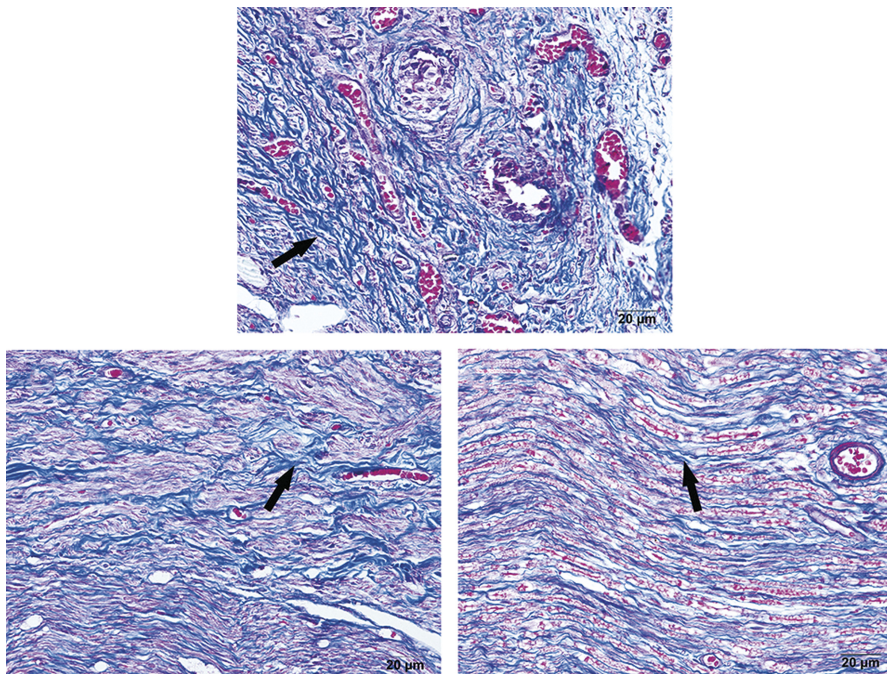


**FIGURE 5.** Results of trichrome Masson's staining. (Above, middle) Dense blue stained collagens with haphazardly arranged nerve fascicles in the control group (black arrow shows the blue collagens). (Below, left) Moderately regenerated collagens in a chaotic pattern in the nonaligned nanofiber group (black arrow shows the blue collagens). (Below, right) Slightly blue stained collagens with relatively orderly arranged nerve fibers in the aligned nanofiber group (black arrow shows the blue collagens).

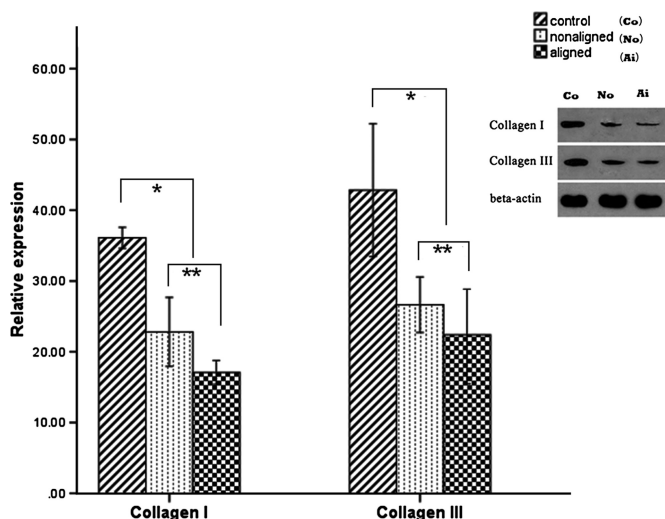


**FIGURE 6.** Results of relative expression of collagen I and collagen III in the neuromas. The protein content of collagens I and III in the control group was significantly higher than that of the 2 capping groups ( $*P < 0.001$ ); in addition, the protein content of collagens I and III of the aligned group was even lower than that of the nonaligned group ( $**P < 0.01$ ).

and  $10.15 \pm 3.08$ , respectively. Significant differences were seen among the 3 groups (all  $P < 0.01$ ) (Fig. 9).

**Ultrastructural Findings by Transmission Electron Microscope**

In each group, the basic structure consisted of a perineurial cell-Schwann cell-axon complex formed by groups of myelinated and unmyelinated axis cylinders surrounded by collagen fibers and

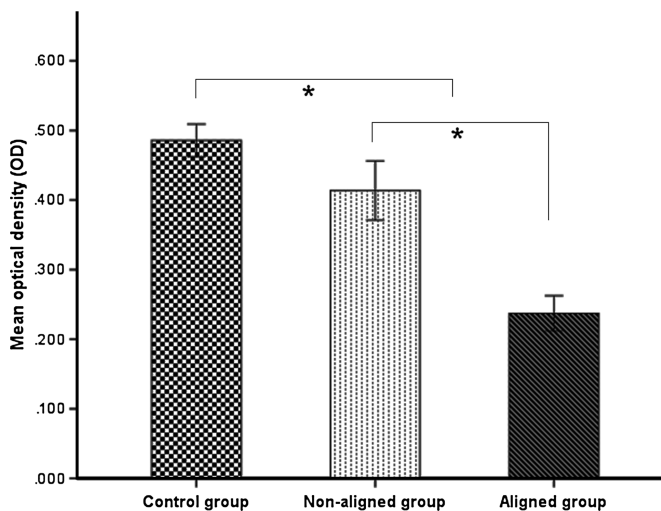


**FIGURE 8.** Results of mean optical density of immunostaining of NF-200. The expression level of NF-200 evaluated by optical density (OD) showed that the aligned group had a minimal OD value of the 3 groups ( $*P < 0.001$ ).

fibroblasts (Fig. 10). However, a much higher ratio of unmyelinated and myelinated fibers was seen in the control group ( $P < 0.001$ ; Fig. 11); the myelin sheath in the aligned group was found to be significantly thicker than that in the control and nonaligned group ( $P < 0.05$ ; Fig. 12).

**DISCUSSION**

Nanofibrous scaffolds generated by electrospinning have been widely investigated and have gained increasing popularity in the field

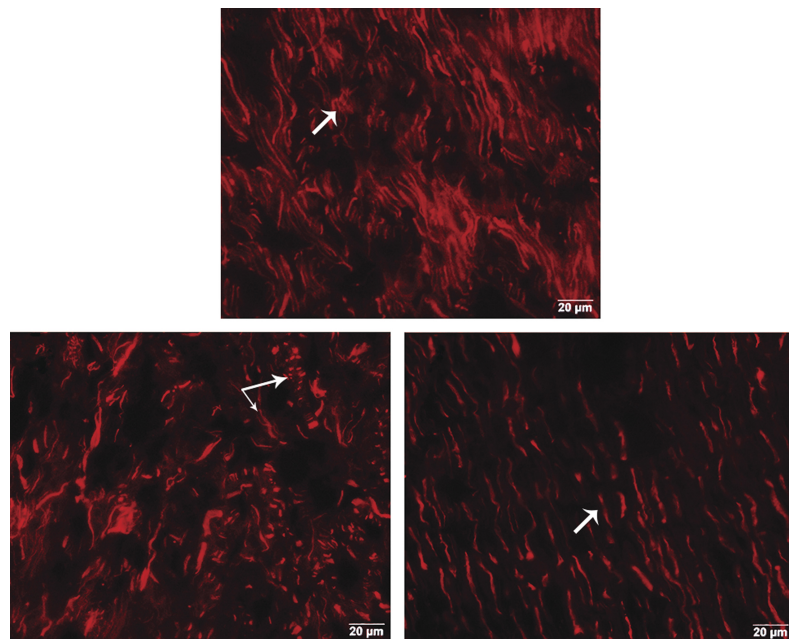


**FIGURE 7.** Results of regenerated nerve fibers labeled by NF-200 using immunofluorescent staining. (Above, middle) In the control group, the larger and medium sizes of axons (marked with NF-200 and stained with TRIC) were densely distributed in a chaotic way. The arrow shows the densely clustered axons. (Below, left) In the nonaligned group, the axons regenerated moderately but also presented a chaotic appearance. The arrows show the transverse and longitudinal axons. (Below, right) In the aligned group, the regenerated axons were arranged regularly in a linear fashion. The arrow shows the regenerated axon.

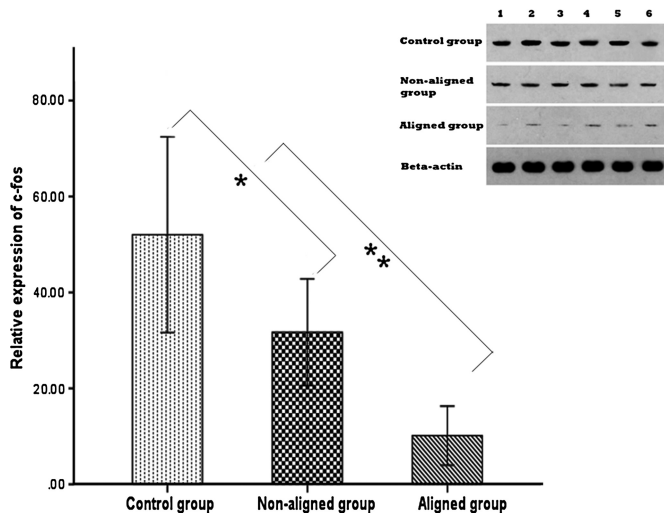


**FIGURE 9.** Results of expression of c-fos in the spinal cord. The expression of c-fos in the L4 lumbar spinal cord, as a pain marker, was significantly decreased in the nonaligned group in comparison with the control group (\* $P = 0.004$ ); furthermore, its expression was even lower in the aligned group than that of the nonaligned group (\*\* $P = 0.002$ ).

of tissue engineering in recently years.<sup>25-27</sup> The features of the extracellular matrix that is critical for tissue regeneration can be achieved using electrospinning technique.<sup>21</sup> Aligned nanofibers were reported to provide contact guidance to cultured cells, resulting in an elongation and alignment of cells along the axes of the fibers.<sup>28-30</sup> The study of Ceballos et al<sup>31</sup> demonstrated that the aligned collagen gels presented an improved template for neurite extension compared with random collagen gels. Our previous study also supported the work of Ceballos et al, showing that the same nerve conduit construct greatly improved the Schwann cell affinity to align in a linear fashion.<sup>21</sup> It has been widely accepted that the pathology of traumatic neuromas is based on admixture of nerve elements and fibrous tissue arranged in a haphazard fashion, which may be the main cause of neuropathic pain.<sup>20</sup> In this research, we observed that well-organized regenerated nerve fibers with a much thicker myelin sheath were only present in the aligned group, indicating that the regenerated nerve fibers in this group were relatively “healthier” compared with those in the other 2 groups. These findings imply that the aligned nanofiber biomaterials may play a unique role in the management of traumatic neuromas.

In clinical practice, the status of pain can be easily expressed by the patients. However, researchers have found that it is difficult to evaluate the effectiveness of methods of pain relief with experimental traumatic neuromas.<sup>17,18</sup> As an alternative, the behavior of autotomy in animals, which is induced by the neurotomy of a peripheral nerve and characterized as a typical behavior of licking, scratching, and self-mutilation of the denervated limb, has been taken as an animal

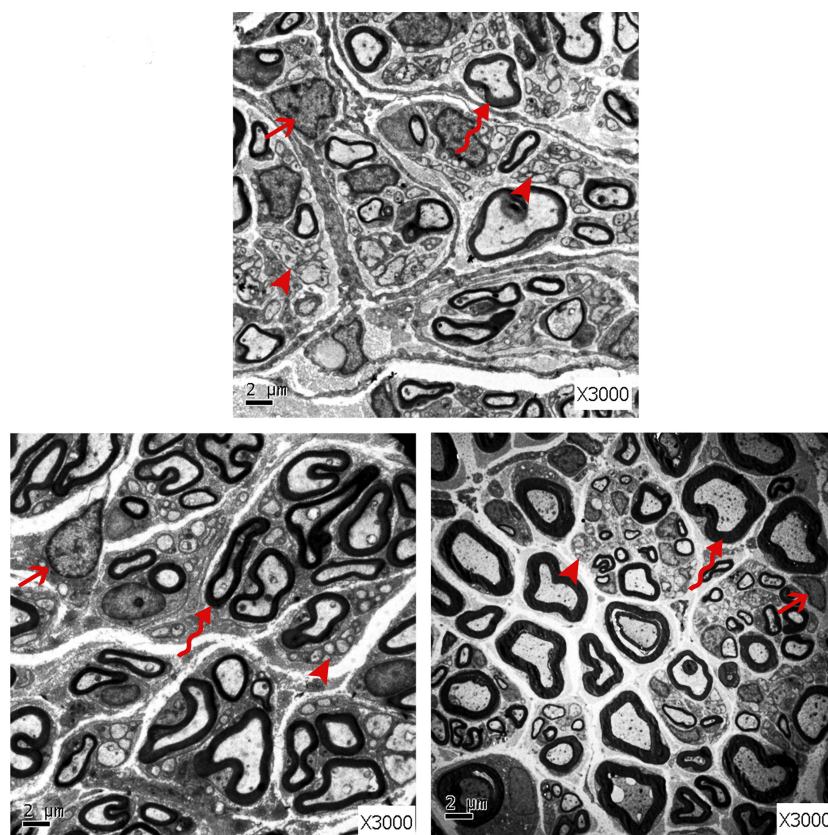


**FIGURE 10.** Ultrastructural observation of the neuromas. (Above, middle) Control group: many unmyelinated fibers and only a few myelinated fibers were seen. The arrow heads show the unmyelinated fibers, the curved arrow shows the myelinated fiber with thin myelin sheath, and the straight arrow shows the fibroblast. (Below, left) Nonaligned group: relatively fewer unmyelinated fibers were seen. The arrow heads show the unmyelinated fibers, the curved arrow shows the myelinated fiber with relatively thicker myelin sheath, and the straight arrow shows the fibroblast. (Below, right) Aligned group: plenty of myelinated fibers were observed. The arrow heads show the unmyelinated fibers, the curved arrow shows the myelinated fiber with thick myelin sheath, and the straight arrow shows the fibroblast.

model of neuropathic pain-related spontaneous sensory disorders, such as anesthesia dolorosa and phantom limb pain.<sup>32,33</sup> In the current study, we found that the autotomy behavior was significantly suppressed in the 2 capping groups in comparison with the control group after 1 week, but no differences in autotomy scores were observed between the 2 capping groups.

Nonetheless, no studies have yet to confirm whether or not the autotomy behavior was directly related to pain.<sup>17</sup> Quantitative evaluation of tactile allodynia<sup>34</sup> or Hargreaves plantar test for thermal hyperalgesia<sup>35</sup> in rat paws may be an optimal method to assess the neuropathic pain of traumatic neuromas for this study; the occurrence of autotomy precludes this approach. To precisely evaluate the pain status of the neuromas, the detection of c-fos level in the spinal cord was performed according to the literature.<sup>17</sup> Studies have revealed that the expression of the c-fos protooncogene in the nuclei of postsynaptic neurons of the spinal cord is a useful marker for neural activity and an indicator of pain caused by transection, ligation, chemical stimuli, and allodynia.<sup>36,37</sup> Therefore, investigation of the expression level of the c-fos protooncogene in the neurons of the spinal cord can provide useful data for evaluating the effectiveness of the capping technique for pain relief from traumatic neuromas. Our findings in the present study showed that the expression level of c-fos in the spinal cord was significantly decreased in the nonaligned group compared with the control group; more importantly, its expression level was even lower in the aligned group than that of the nonaligned group, indicating that the aligned nanofiber conduit is superior to the nonaligned one in suppressing the pain caused by nerve amputation. The fact that no significant difference in autotomy scores was seen between the 2 capping groups may imply that the autotomy behavior might be a rough response to neuropathic pain, which could not be distinguished precisely or might not be a reliable pain marker in the evaluation of painful neuroma, and further studies are warranted to verify these hypotheses.

The ratio of myelinated and unmyelinated fibers plays a critical role in the pathological features of traumatic neuromas.<sup>38–40</sup> The general appearance of the regenerated nerve fibers in a painful neuroma is characterized with innumerable minuscule nerve fascicles including a considerably larger number of unmyelinated fibers than myelinated fibers.<sup>41</sup> The results of transmission electron microscopy in this study showed that there were more unmyelinated fibers in the control group and nonaligned group than in the aligned group. Because pain is mainly

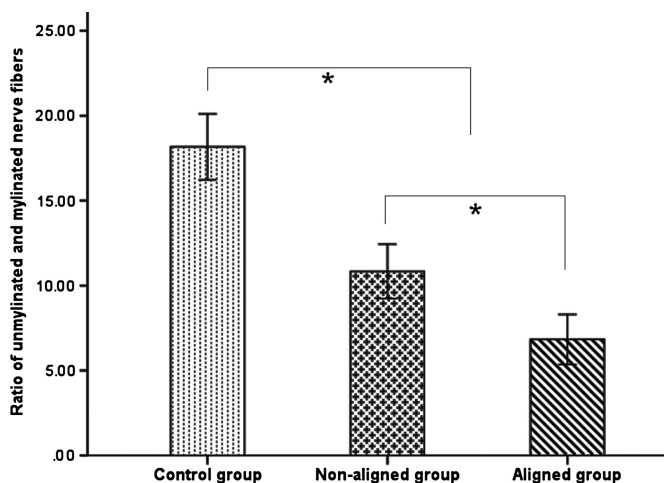


**FIGURE 11.** Ratio of unmyelinated and myelinated nerve fibers. The ratio of unmyelinated and myelinated nerve fibers in the aligned group was the lowest among the 3 groups (\*  $P < 0.001$ ).

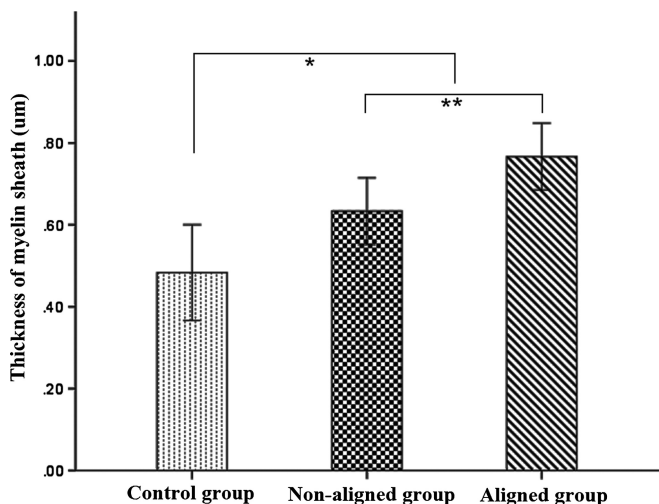


**FIGURE 12.** The myelin sheath thickness of each group. The myelin sheath thickness in the aligned group was the thickest among the 3 groups (\* $P = 0.002$ , \*\* $P = 0.004$ ).

mediated by unmyelinated nerve fibers,<sup>2,42</sup> these findings indicate additional advantage of aligned nanofiber conduits for the management of painful neuromas.

Another essential parameter for the evaluation of neuroma prevention is the extent of neuroma growth. Koch et al<sup>24</sup> used the maximum diameter of the neuroma as an index for quantitative analysis. As known, neuroma growth is tridimensional; therefore, the assessment of the neuroma can only be partially achieved by a determination of its diameter. In this research, a WR was adopted as a quantitative value. Thus, the general regeneration status of the neuroma can be assessed. A maximal WR was found in the control group. We were surprised to find that the aligned group had a significant lower WR when compared with the nonaligned group. Furthermore, the regeneration of collagens I and III was significantly inhibited in the aligned group in contrast to the control group and the nonaligned group. In addition, this tendency was also seen in terms of the regeneration extent of nerve fibers with the fewest newborn axons observed in the aligned group. These results indicate the potential advantage of the aligned nanofiber biomaterial in prevention of neuroma formation.

In conclusion, the aligned nanofiber conduits can significantly facilitate linear nerve regeneration, inhibit neuroma growth, and reduce neuropathic pain after neurectomy. The aligned nanofibers might be a preferred biomaterial for the prevention or treatment of painful amputated neuromas, and a new treatment strategy using aligned biomaterial conduits may be warranted.

#### ACKNOWLEDGMENT

The authors give special thanks to Jon Kolkin, M.D. for his assistance in the editing of this manuscript and the medical statistician Jingwei Zheng for the completion of statistical analysis.

#### REFERENCES

- Mathews GJ, Osterholm JL. Painful traumatic neuromas. *Surg Clin North Am.* 1972;52:1313–1324.
- Zimmermann M. Pathobiology of neuropathic pain. *Eur J Pharmacol.* 2001; 429:23–37.
- Bowsher D. Human “autotomy”. *Pain.* 2002;95:187–189.
- Niederberger E, Kuhlein H, Geisslinger G. Update on the pathobiology of neuropathic pain. *Expert Rev Proteomics.* 2008;5:799–818.
- Harden RN. Chronic neuropathic pain. Mechanisms, diagnosis, and treatment. *Neurologist.* 2005;11:111–122.

6. Farley HH. Painful stump neuroma—treatment of. *Minn Med*. 1965;48:347–350.
7. Tupper JW, Booth DM. Treatment of painful neuromas of sensory nerves in the hand: a comparison of traditional and newer methods. *J Hand Surg Am*. 1976;1:144–151.
8. Mass DP, Ciano MC, Tortosa R, et al. Treatment of painful hand neuromas by their transfer into bone. *Plast Reconstr Surg*. 1984;74:182–185.
9. Kirvela O, Nieminen S. Treatment of painful neuromas with neurolytic blockade. *Pain*. 1990;41:161–165.
10. Herbert TJ, Filan SL. Vein implantation for treatment of painful cutaneous neuromas. a preliminary report. *J Hand Surg Br*. 1998;23:220–224.
11. Krishnan KG, Pinzer T, Schackert G. Coverage of painful peripheral nerve neuromas with vascularized soft tissue: method and results. *Neurosurgery*. 2005;56(suppl 2):369–378.
12. Gould JS, Naranje SM, McGwin G Jr, et al. Use of collagen conduits in management of painful neuromas of the foot and ankle. *Foot Ankle Int*. 2013;34:932–940.
13. Vernadakis AJ, Koch H, Mackinnon SE. Management of neuromas. *Clin Plast Surg*. 2003;30:247–268, vii.
14. Wu J, Chiu DT. Painful neuromas: a review of treatment modalities. *Ann Plast Surg*. 1999;43:661–667.
15. Galeano M, Manasseri B, Risitano G, et al. A free vein graft cap influences neuroma formation after nerve transection. *Microsurgery*. 2009;29:568–572.
16. Koch H, Haas F, Hubmer M, et al. Treatment of painful neuroma by resection and nerve stump transplantation into a vein. *Ann Plast Surg*. 2003;51:45–50.
17. Sakai Y, Ochi M, Uchio Y, et al. Prevention and treatment of amputation neuroma by an atelocollagen tube in rat sciatic nerves. *J Biomed Mater Res B Appl Biomater*. 2005;73:355–360.
18. Okuda T, Ishida O, Fujimoto Y, et al. The autotomy relief effect of a silicone tube covering the proximal nerve stump. *J Orthop Res*. 2006;24:1427–1437.
19. Kakinoki R, Ikeguchi R, Matsumoto T, et al. Treatment of painful peripheral neuromas by vein implantation. *Int Orthop*. 2003;27:60–64.
20. Williams HB. The painful stump neuroma and its treatment. *Clin Plast Surg*. 1984;11:79–84.
21. Wang CY, Zhang KH, Fan CY, et al. Aligned natural-synthetic polyblend nanofibers for peripheral nerve regeneration. *Acta Biomater*. 2011;7:634–643.
22. Zhang K, Wang H, Huang C, et al. Fabrication of silk fibroin blended P(LLA-CL) nanofibrous scaffolds for tissue engineering. *J Biomed Mater Res A*. 2010;93:984–993.
23. Zeltser R, Beilin B, Zaslansky R, et al. Comparison of autotomy behavior induced in rats by various clinically-used neurectomy methods. *Pain*. 2000;89:19–24.
24. Koch H, Herbert TJ, Kleinert R, et al. Influence of nerve stump transplantation into a vein on neuroma formation. *Ann Plast Surg*. 2003;50:354–360.
25. Beilke MC, Zewe JW, Clark JE, et al. Aligned electrospun nanofibers for ultrathin layer chromatography. *Anal Chim Acta*. 2013;761:201–208.
26. Xu Y, Wu J, Wang H, et al. Fabrication of electrospun poly(L-lactide-co-ε-caprolactone)/collagen nanofiber network as a novel, three-dimensional, macroporous, aligned scaffold for tendon tissue engineering. *Tissue Eng Part C Methods*. 2013;19:925–936.
27. Wang CY, Liu JJ, Fan CY, et al. The effect of aligned core-shell nanofibers delivering NGF on the promotion of sciatic nerve regeneration. *J Biomater Sci Polym Ed*. 2012;23:167–184.
28. Corey JM, Lin DY, Mycek KB, et al. Aligned electrospun nanofibers specify the direction of dorsal root ganglia neurite growth. *J Biomed Mater Res A*. 2007;83:636–645.
29. Wang HB, Mullins ME, Cregg JM, et al. Creation of highly aligned electrospun poly-L-lactic acid fibers for nerve regeneration applications. *J Neural Eng*. 2009;6:016001.
30. Prabhakaran MP, Vatankhah E, Ramakrishna S. Electrospun aligned PHBV/collagen nanofibers as substrates for nerve tissue engineering. *Biotechnol Bioeng*. 2013;110:2775–2784.
31. Ceballos D, Navarro X, Dubey N, et al. Magnetically aligned collagen gel filling a collagen nerve guide improves peripheral nerve regeneration. *Exp Neurol*. 1999;158:290–300.
32. Wall PD, Devor M, Inbal R, et al. Autotomy following peripheral nerve lesions: experimental anaesthesia dolorosa. *Pain*. 1979;7:103–111.
33. Coderre TJ, Grimes RW, Melzack R. Deafferentation and chronic pain in animals: an evaluation of evidence suggesting autotomy is related to pain. *Pain*. 1986;26:61–84.
34. Chaplan SR, Bach FW, Pogrel JW, et al. Quantitative assessment of tactile allodynia in the rat paw. *J Neurosci Methods*. 1994;53:55–63.
35. Hirose K, Iwakura N, Orita S, et al. Evaluation of behavior and neuropeptide markers of pain in a simple, sciatic nerve-pinch pain model in rats. *Eur Spine J*. 2010;19:1746–1752.
36. Kajander KC, Madsen AM, Iadarola MJ, et al. Fos-like immunoreactivity increases in the lumbar spinal cord following a chronic constriction injury to the sciatic nerve of rat. *Neurosci Lett*. 1996;206:9–12.
37. Siddall PJ, Xu CL, Floyd N, et al. C-fos expression in the spinal cord of rats exhibiting allodynia following contusive spinal cord injury. *Brain Res*. 1999;851:281–286.
38. Carlton SM, Dougherty PM, Pover CM, et al. Neuroma formation and numbers of axons in a rat model of experimental peripheral neuropathy. *Neurosci Lett*. 1991;131:88–92.
39. Muehleman C, Rahimi F. Effectiveness of an epineurial barrier in reducing axonal regeneration and neuroma formation in the rat. *J Foot Surg*. 1990;29:260–264.
40. Wall PD, Gutnick M. Ongoing activity in peripheral nerves: the physiology and pharmacology of impulses originating from a neuroma. *Exp Neurol*. 1974;43:580–593.
41. Cravioto H, Battista A. Clinical and ultrastructural study of painful neuroma. *Neurosurgery*. 1981;8:181–190.
42. Collins WR Jr, Nulsen FE, Randt CT. Relation of peripheral nerve fiber size and sensation in man. *Arch Neurol*. 1960;3:381–385.